MODEL OF RED BLOOD CELL ROTATION IN THE FLOW TOWARD A CELL SIZING ORIFICE

APPLICATION TO VOLUME DISTRIBUTION

M. O. BREITMEYER, E. N. LIGHTFOOT, *and* W. H. DENNIS

From the Department of Biological Engineering, Rose Polytechnic Institute, Terre Haute, Indiana 47803, and the Department of Chemical Engineering and Physiology, University of Wisconsin, Madison, Wisconsin 53706

ABSTRACT The rotation of human red blood cells (RBC) as they flow in the shear field established by a Coulter type orifice is modeled. This model, based on hydrodynamics of ellipsoid rotation in laminar creeping flow, is used to calculate the probability of the cells entering the orifice with a specific orientation. The electrical resistance change produced by a cell passing through the orifice of an electronic cell volume detector is the product of an orientation-dependent shape factor and the cell volume. This paper presents a method to calculate the shape factor probability distribution which can be used to predict its effect on the cell volume distribution. Experimental results confirm the theoretical prediction that the right skewness of resistance change distributions is in part a result of the nonspherical shape of red cells.

INTRODUCTION

The number and size of particles suspended in an electrolyte solution is often estimated by measuring the electrical resistance changes that occur when these particles move through a small orifice, for example, in a Coulter counter. Many reports exist which describe the application of this technique to cells, mammalian and bacterial, or emulsions of nonelectrolytes. Some of these cells are not spherical; in particular the RBC is normally a biconcave oblate spheroid. When a nonspherical particle moves in the shear field established by fluid flow through a circular orifice, the particle will rotate or tumble; consequently all particles will not have the same orientation (thus shape factor) when they reach the orifice. A theoretical relationship between volume V, resistance change ΔR, and shape factor f is

$$\Delta R = kfV, \tag{1}$$

where k is a constant which depends on orifice and fluid characteristics (1). Since resistance change is proportional to the product of particle volume and an orientation-dependent shape factor, measured ΔR distributions must be corrected for variation in orientation to obtain true volume distributions. This paper deals specifically with human RBC resistance and volume distributions.

Many investigators have reported RBC volume distributions (actually ΔR distributions) which are skewed in the direction of larger cell volume (2, 3) or are bimodal (4). Instrument bias can cause skewness (5); however, all of the experimental data cannot be explained by variation in residence time (2). Optical estimates of volume (Price-Jones curves) lead to gaussian distributions. Recently Gutmann (6) stated that the observed asymmetry could be explained by assuming cells to take one of two extreme orientations in passing through the orifice.

The purpose of the present paper is to describe this asymmetry directly in terms of cell shape and system hydrodynamics. More specifically a useful relation for the frequency distribution of RBC orientation based on the hydrodynamics of ellipsoid rotation in a shear field will be developed. It will be shown that there is a continuous distribution of orientations rather than the simple discontinuous two-orientation model of Gutmann. Explicit relations are given for the specific case of normal human RBC. Extension to cells of other shapes of revolution is straightforward.

METHODS

A 100 μ ($2r$) diameter orifice (Coulter Electronics, Industrial Div., Hialeah, Fla.) was used in conjunction with the electronics from the RIDL (Radiation Institute Development Laboratory, Des Plaines, Ill.) particle-sizing system. Pressure drop, ΔP, across the orifice was con-

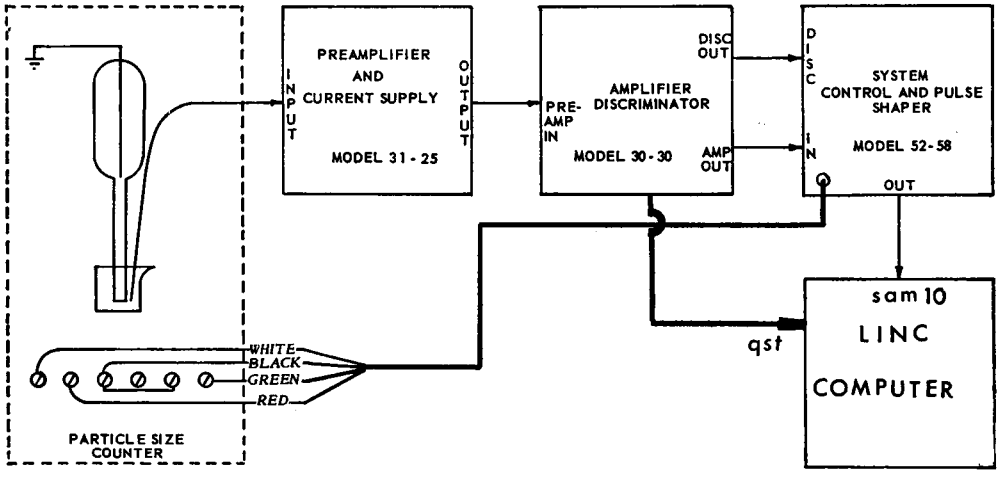

FIGURE 1 Block diagram of cell sizing system. Electrodes are shown on either side of the glass tube in which an orifice (diameter = 100 μ) is embedded. The discriminator triggers the LINC via quick restart (qst) to stop and wait for a pulse from the pulse shaper to the analogue sample line 10 (sam 10).

stant at 162 mm Hg. Direct current (0.5 ma), flowing through the orifice from external to internal electrode, changed each time the resistance of the orifice was altered by a particle passing through it. In the preamplifier this current variation produced a voltage pulse. As shown in Fig. 1 the shaped voltage-output pulses from the RIDL system entered an analogue sampling line of a LINC computer (Digital Equipment Corp., Maynard, Mass.) which was programmed as a 256 channel analyzer. Resistance distributions were visually displayed as histograms (number of particles producing a given ΔR vs. ΔR, Fig. 7) several seconds after a suspension of cells was sampled; these data were also stored on magnetic tape. The mean or number average resistance change, $\overline{\Delta R} = (\sum n_i(\Delta R)_i / \sum n_i$, where n_i = number of cells, and the total number of particles in a histogram were also part of the display. The computer was programmed to sample the same number of particles (7000) for each histogram, or to sample for a constant volume (0.5 ml). Distributions containing 20,000 samples were compared to those containing 7000 taken under identical conditions. See reference 7 for evaluation and description of instrumentation.

Resistance distributions of human RBC, drawn in heparin, thrice washed, and then suspended in Abbott isotonic saline (C. W. Abbott & Co., Inc., Baltimore, Md.) (T = 22°C, pH = 7.2, dilution blood:saline, 1:60,000) was compared to resistance distributions of RBC from the same cell population sphered by adding saponin (0.25 ppm) and to cells restored to original discoid shape by addition of serum of the original blood sample.

THEORY

To determine the effect of orientation on the resistance distribution it is first necessary to determine the frequency distribution of orientations of particles as they enter the orifice. This in turn requires knowledge of flow patterns in the system and their effect on particle orientation. One must then relate orientation to shape factor f in equation 1, and determine the probability of a given f. Finally it would be desirable to devise a means of predicting the volume distribution from the observed resistance distribution. Solution of these problems is described briefly in this section.

Approximate Characterization of the Flow Field in the Neighborhood of the Orifice

The orifice region of the apparatus used is described pictorially in Fig. 2. The orifice diameter $2r$ is approximately 100 μ and the thickness or the orifice plate is 100 μ. In approximating the flow field the thickness of the orifice plate was neglected and the effective RBC orientation was taken to be that as its center of mass enters the plane of the orifice. It is further assumed that laminar creeping flow exists upstream from the orifice. It is believed by the authors that a more refined model is not presently justified in view of the uncertainties in electrical resistance measurements. In any event the analysis outlined below is intended as only a first-order correction to the presently used method of estimating volume distributions.

The velocity profile system is

$$u = \delta(3q/2\pi r^2) \cos^2 \eta/(\cosh \xi \, (\cosh^2 \xi - \sin^2 \eta)^{1/2}), \qquad (2)$$

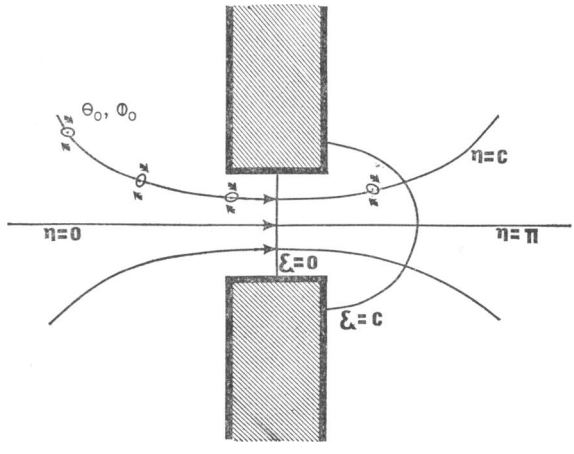

FIGURE 2 Idealized schematic of the orifice and the coordinate system showing the orifice in cross section (note in the mathematical model the orifice was assumed to be infinitely thin and only the upstream region was considered), the oblate spheroidal coordinates xi (ξ) and eta (η), and the streamlines of constant η on which the discoid red cells tumble as they flow from some initial random position and orientation (θ_0 and ϕ_0).

where the oblate spheroidal coordinates η and ξ are defined by Happel and Brenner (8) (see Fig. 2). All other velocity components are assumed to be zero. These coordinates are related to cylindrical coordinates by

$$z = r \sinh \xi \cos \eta; \quad \rho = r \cosh \xi \sin \eta. \tag{3}$$

It can be seen that the flow is axisymmetric and entirely in the ξ direction. The shear rate may then be expressed as

$$g(\xi, \eta) = h_\eta \frac{\partial u_\xi}{\partial \eta}, \tag{4}$$

and

$$g = -(3q/2\pi r^3) \sin \eta \cos \eta/(\cosh \xi (\cosh^2 \xi - \sin^2 \eta)^{1/2})$$
$$(2 - (\cos^2 \eta/\cosh^2 \xi - \sin^2 \eta)). \tag{5}$$

The above equations are reliable only in the neighborhood of the orifice, but, since shear rate drops off very rapidly with distance, only this region need be considered. To show this the extent of rotation is defined as

$$E = \int_0^t g(t)dt, \tag{6}$$

in accordance with Burgers (9). In principle the shear rate appearing in this expres-

sion should be a weighted average over the region occupied by the particle. For all practical purposes, it is satisfactory to use the value of g at the particle center of mass. That is, the radius of curvature of the streamlines can be considered large relative to the thickness of the cell.

Since isolated RBC settle slowly in saline they will very nearly follow the fluid streamlines. We may, therefore, approximate the extent of rotation as

$$E = \int_0^{\xi_0} (\sin \eta / \cos \eta)(2 - (\cos^2 \eta / (\cosh^2 \xi - \sin^2 \eta)))\partial\xi. \qquad (7)$$

Examination of this equation shows that E is of the order ξ_0, the value of ξ at which the particle enters the system. For the apparatus used $\xi_0 \gg 1$. It follows that the time-averaging techniques reviewed in Burgers (9) are valid and that the probability of a given orientation at the orifice is very nearly the same as for long-continued shear at an arbitrary uniform rate.

Orientation Probabilities for an Ellipsoid in a Uniform Shear Field

The rotation of ellipsoids in a shear field was first studied by Jeffery (10). This and other pertinent work have since been summarized by Burgers (9), who used the coordinate system shown in Fig. 3, and the velocity field

$$u = \delta_x g y. \qquad (8)$$

The line OM shown in this figure represents one-half of the axis of rotation of the RBC under consideration. The instantaneous orientation of the cell is specified by the two angles ϕ and θ. These angles will in turn be functions of t which is time, since the start of tumbling, the initial orientation (ϕ_0, θ_0) at $t = 0$, and the rate of shear g:

$$\tan \phi = (a/b) \tan (gabt/(a^2 + b^2)), \; 0 \leq t \leq T, \qquad (9)$$

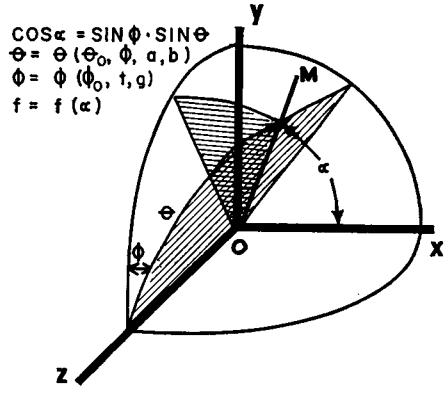

FIGURE 3 The spherical coordinate system of Burgers (9) is used to relate the spatial orientation (α) of the circular axis (OM) of a particle to the spherical angles θ and ϕ. The yz plane contains the plane of the orifice and the x axis is the centerline of the orifice. Positive flow is in the direction of positive x.

$$\tan^2 \theta = (a^2 \cos^2 \phi_0 + b^2 \sin^2 \phi_0) \tan^2 \theta_0 / (a^2 \cos^2 \phi + b^2 \sin^2 \phi), \quad (10)$$

$$T = 2\pi(a^2 + b^2)/gab. \quad (11)$$

Here a and b are the half-axes of the ellipsoid of revolution used to approximate the RBC shape (see Fig. 4).

The probability of a given orientation at the orifice will be approximately that obtained from equations 9–11 if the radii of curvature of streamlines are large compared to a and b. This condition should be met to a satisfactory degree, in particular because most of the flow will be in the central regions of the orifice where the curvature is slight.

We may then consider our curved streamlines to be effectively straight at the orifice with OX perpendicular to the plane of the opening. It follows from the symmetry of the blood cell that its electrical resistance is determined by the single angle α between

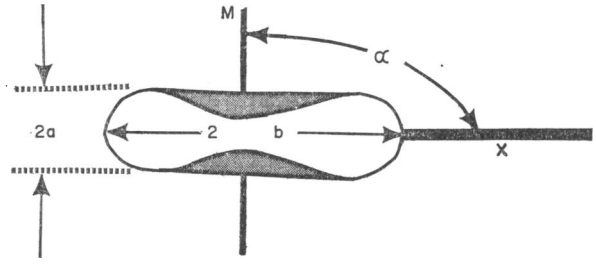

FIGURE 4 Cross section of RBC (biconcave disc) where 2 a is the maximum thickness and 2 b the diameter. The spatial angle α relates the circular axis OM to the x axis of Fig. 3.

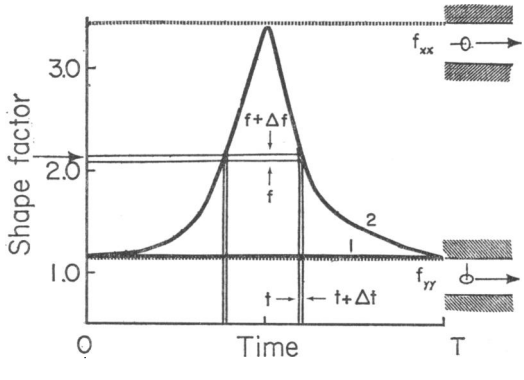

FIGURE 5 Two of the curves which give shape factor f as a function of time (t) during period of rotation (T), for a constant θ_0 and ϕ_0. The dotted lines represent the minimum shape factor (f_{yy}, $\alpha = \pi/2$, cell axis along the z or y axis) and the maximum shape factor ($f_{zz}, \alpha = 0$, cell axis OM parallel to x axis). In curve 1 ($\theta_0 = 0$) there is no change in f since the cell simply rolls toward the orifice from its initial position, its axis OM always parallel to OZ. In curve 2 $\theta_0 = \pi/2$, f varies from minimum to maximum since the cell tumbles through a full 180°.

OM and *OX*. It may also be seen that

$$\cos \alpha = \sin \phi \sin \theta. \tag{12}$$

It remains to determine the relation between α and the shape factor f. This relation can be obtained easily from the theory of conduction through an isotropic medium (11). Under these conditions

$$f = f_{vv} - \cos^2 \alpha (f_{vv} - f_{xx}), \tag{13}$$

where f_{xx} and f_{vv} are the shape factors for orientations in which the RBC axis, *OM*, is parallel or perpendicular to the streamlines. (See inserts at right in Fig. 5).

CALCULATIONS

To permit explicit calculations the RBC was assumed to tumble like an oblate ellipsoid with half-axes $a = 1.2$ and $b = 4.3$ μ. Shape factors were taken as $f_{vv} = f_{zz} = 1.174$ and $f_{xx} = 3.365$ from Velick (12) for ellipsoids of axis ratios 4:4:1. Results of the calculations discussed below are not highly sensitive to these choices.

With the shear rate calculated from equation 5, $\xi = 0$, $\eta = \pi/4$, $r = 50$ μ, and $q = 0.035$ ml/sec, equations 9–13 were used to generate a family of shape-factor–time relations $f(t)$ with θ_0 as a parametric variable. Two such curves, for $\theta_0 = 0$ and $\pi/2$, are shown in Fig. 5. Note that it is not necessary to consider variations in ϕ_0 since the value of ϕ_0 will not affect the proportion of time spent by the cell at any α over a large number of cycles.

If all values of θ_0 are assumed to be equally probable; that is, that the cells enter the flow system with a random orientation, it is then possible to estimate the fractional probability for any given orientation as

$$dP(f) = \frac{\Delta t_f}{T}, \tag{14}$$

where $dP(f)$ = fractional probability of a given shape factor between f and $f + \Delta f$ when cells reach the orifice plane, Δt_f = time spent by a cell in orientations corresponding to shape factors between f and $f + \Delta f$, averaged with respect to θ_0, T = time for one revolution, independent of both θ_0 and ϕ_0.

15 shape-factor–time relations of the type shown in Fig. 5 were calculated for evenly spaced θ_0 between 0 and $\pi/2$. Each curve depicts the change in f during one-half revolution of the cell. The two curves of Fig. 5 represent the extremes of possible behavior. Cells with an initial orientation $\theta_0 = 0$ "roll" along the fluid streamlines without change in effective orientation; these always have the orientation corresponding to minimum resistance. Those with $\theta_0 = \pi/2$ on the other hand take all possible orientations. It is clear from the nature of the tumbling process that changes occur most rapidly at orientations corresponding to maximum resistance

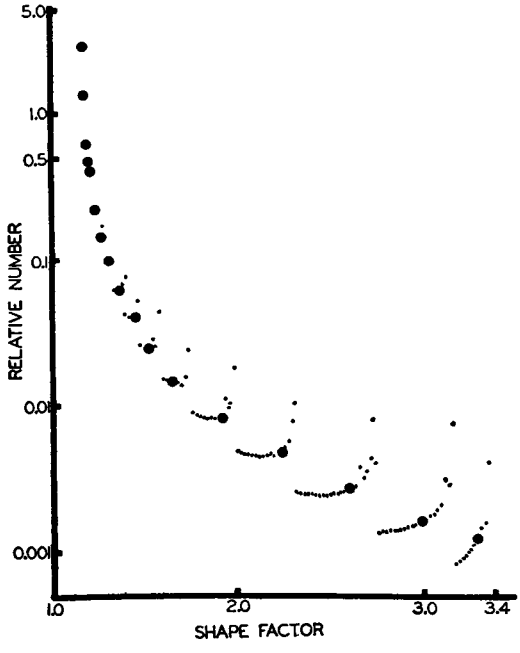

FIGURE 6 Frequency distribution of shape factor calculated by summing the fractional probabilities of each shape factor (Fig. 5). The large points represent the average value of $P(f)$; the small points are the individual results of the numerical summation.

and least rapidly at those corresponding to minimum resistance. As a result, the probability of a given orientation falls off with increase in the corresponding f value. To estimate these probabilities each of the 15 shape-factor–time relations were divided in increments of 0.005 on the f axis. Then the total probability of each f was calculated as proportional to the time spent in each of these shape-factor ranges. This relatively fine grid was required for the results to be useful in subsequent numerical integration procedures. It may be seen from Fig. 6 that the contribution of cells offering a higher than minimum shape factor is appreciable. The cyclic nature of the $P(f)$ values in these results stems from the method of numerical summation.

EXPERIMENTAL RESULTS

The ΔR frequency distribution for a suspension human RBC was skewed to the right (Fig. 7 A). Many workers interpret this as indicating a relatively greater number of large cells. Each histogram represented 7,000 individual measurements of ΔR. The standard deviation of $\bar{\Delta}R$ (mean) of 35 distributions measured from one population of RBC was less than 2%. Furthermore, these distributions could be considered identical with greater than 90% confidence, as determined by a chi-squared test. Each bar of the histogram represents the average of two channels of the 256-channel analysis of ΔR; that is, the maximum channel represented in Fig. 7 D is 128 units.

The sketch in Fig. 8 depicts the transformation of discoid red cells to crenated

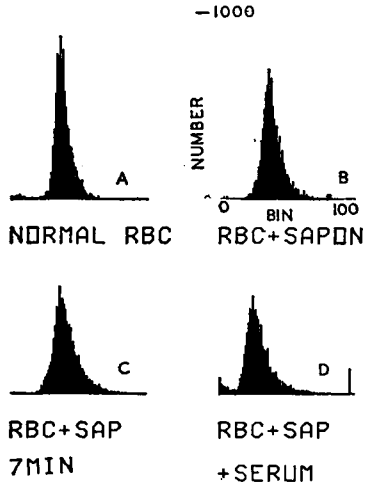

FIGURE 7 Histograms (number of cells producing a given resistance change vs. resistance change (0 to 100 bins) drawn by LINC computer. A. Normal RBC (1:60,000 dilution in isotonic NaCl). B. Same cells plus saponin 0.25 ppm 4 min after saponin first added. Cells sphere. C. After 7 min. D. Saponin + cells + serum (plasma proteins cause cells to become discoid again).

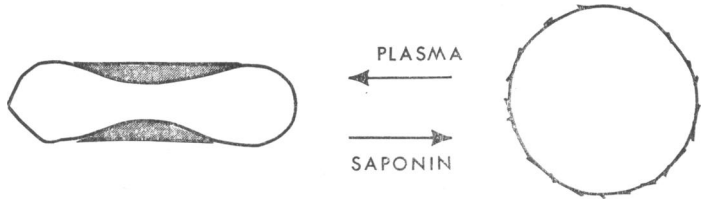

FIGURE 8 Schematic of RBC in saline and red cells + saponin after 10 min.

spheres (12) when saponin was added (0.25 ppm). The resistance distribution of these cells 4 and 7 min after addition of saponin shows less skewness or a more normal distribution. (Fig. 7 B, C). The probability of the control distribution, A, and the distribution with saponin, C, being identical was less than 0.5% as determined by the chi-squared test. This result was seen in four other experiments. Increasing the total number of cells sampled or decreasing the cell concentration did not alter the fact that saponin caused the distribution to be less skewed. (Saponin decreased the total cell count by less than 5%.) With the addition of serum containing plasma proteins (also platelets and white cells) the red cells return to the discoid shape (12). Under these conditions ΔR is as seen in Fig. 7 D and has the general characteristics of Fig. 7 A, that is, the initial distribution of normal discoid cells.

DISCUSSION

Three aspects of this paper should be discussed: the relationship between shape-factor distributions and the measured ΔR distributions, pertinent data to include when presenting experimental observations dealing with the Coulter type orifices, and the experimental results of this paper.

If one assumes that the true volume of RBC is normally distributed, it is obvious

from equation 1 and the results presented in Fig. 6 that the resistance change distribution would be skewed to the right. When gaussian volume distributions are multiplied by this shape-factor distribution the frequency distribution of the product is right-skewed. When right-skewed ΔR distributions are divided by the shape-factor distribution, relatively gaussian distributions of volume result.[1]

It must be remembered that the results in this paper are limited in several ways. The shape-factor distribution was obtained under specific conditions: for hypothetical ellipsoidal-shaped RBC with given dimensions entering the orifice on a given streamline $\eta = 45°$, for a specified orifice diameter and flow rate, and for those cells only in the center plane of the orifice. None of these assumptions appears to be severely limiting, and an extension of the model to cover other conditions can be made.

For data obtained with the Coulter type orifice to be meaningful several important parameters should be included with all data reported: the flow rate through the orifice q, the radius of the orifice r, the length of the orifice L, and the cell shape, i.e., in the case of RBC, the half-axes a and b.

Harvey (5) attributed skewness to instrument bias resulting from the particle transit time in the orifice being much less than the rise time of the input amplifier.

The RIDL instrument has a rise time of less than 20 μsec. Since the transit time in this study was 24 μsec, instrument bias should not contribute to skewness.

Although the experimental ΔR distribution for normal red cells (Fig. 7 A) does not display a right notch which characterized distribution determined with a 50 μ orifice (4), there is a definite right skewness. When the cumulative frequency is plotted against ΔR on probability paper (Fig. 9) the deviation from a normal curve can be seen. Saponin (0.25 ppm) caused a noticeable change in the distribution at 4 min and a definite difference at 7 min (Figs. 7 B and C). This is to be expected since saponin at the concentration causes sphering of the red cells with little change in cell volume (12). The difference in the distributions (A to C) can be seen more easily in the probability plot (Fig. 9); the saponin caused the cells to be more normally distributed while the mean resistance (at 50%) increased by only 6%. The small increase in mean resistance is not surprising since f for spherical cells is 1.5 (12); this is slightly larger than the mean f for discoid cells. Cell concentration dropped by less than 5%, thus the alteration of the distribution was principally from the change in shape rather than the relative number of cells of a given size.

Another indication of this dependence of resistance distribution on the shape of red cells occurs when RBC are suspended in hypotonic saline (0.6% NaCl). This treatment produced a gaussian distribution (6). This is in agreement with our results. Gutmann (6) concluded that only two orientations were possible, the minimum and

---

[1] Breitmeyer, M. O., and M. Waldon. 1969. 8th Annual International Conference on Engineering in Medicine and Biology. Chicago. Paper in preparation.

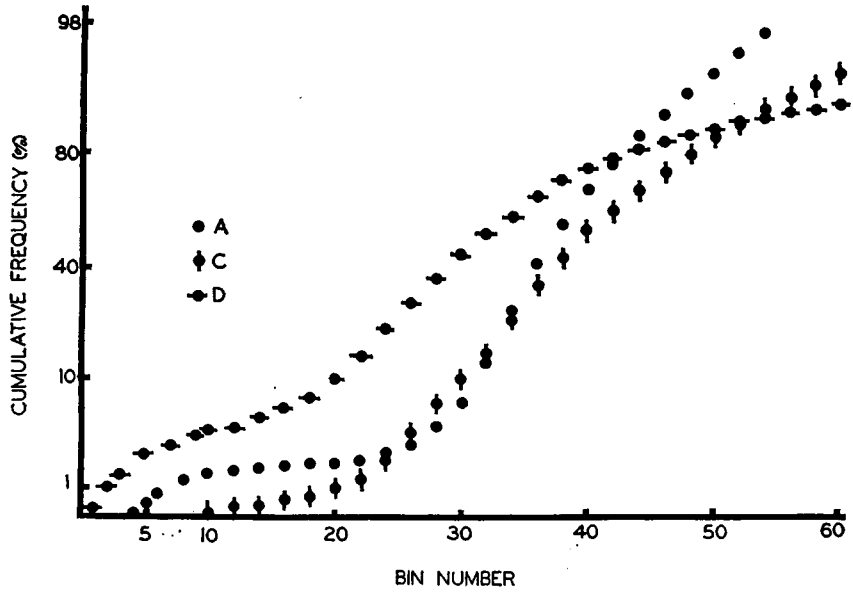

FIGURE 9 Cumulative frequency plot of the data in Fig. 7 A and C. The abscissa is in relative resistance units or bin number. A straight line would result from a perfectly normally distributed histogram. Note the deviations from linearity before and after saponin addition (A and D).

maximum. His conclusion was based on the assumption that cells rotated in the measurement field. Calculation shows the cell to rotate only 5% in passing through the orifice. The experimental evidence and final conclusion do not differ; that is, our work is a refinement and extension of Gutmann's conclusions. However, we make an a priori prediction and do not need empirical constants. Furthermore our equations can be applied to cells of other shapes.

Preliminary data from a recently developed technique which produces 2 μ resolution microholograms[2] of the red cells as they move toward the orifice indicates the model predictions are conservative. That is, the experimentally determined shape-factor distribution has 10% of the cells entering the orifice with a maximum value of 3.3.

This work was supported by grant NSF-GK-3601.

Received for publication 1 June 1970.

TABLE OF SYMBOLS

a	Half-minor axis of ellipsoid (μ).
b	Half-major axis of ellipsoid (μ).

[2] Breitmeyer, M. O., and M. K. Sambandam. 1970. Holographic Record of Moving Red Blood Cells in the Shear Field of Circular Orifice. Meeting of Association for Advancement of Medical Instrumentation, Los Angeles. Manuscript in preparation.

k Orifice coefficient.
E Extent of rotation.
f Shape factor.
g Shear rate (sec^{-1}).
h Metrical coefficient (8).
n Number of observations.
O Origin of rectilinear coordinate system.
ΔP Pressure drop across orifice (mm Hg).
$P(j)$ Probability of j.
q Flow rate (ml/sec).
r Orifice radius (cm).
ΔR Resistance change (Ω).
t Time (sec).
t_L Residence time in orifice = $(L/q)\pi r^2$ (sec).
T Period of revolution (sec).
TT Total time of travel (sec).
u Velocity (cm/sec).
V Volume (μ^3).
x, y, z Rectilinear coordinates.
α Spatial angle between O_x and O_m.
δ Unit vector normal to surface.
η, ξ Oblate spheroidal coordinates (Fig. 2).
θ, ϕ Spherical coordinates (Fig. 3).
π 3.1415.
ρ Density (g/cc).
μ Viscosity (centipoise).

REFERENCES

1. GREGG, E. C., and K. DAVID STEIDLEY. 1965. *Biophys. J.* **5**:393.
2. BASMANN, N. J., B. GLASCOCK, and C. C. LUSHBAUGH. 1962. *Blood J. Hematol.* **20**:241.
3. WILKINS, B., J. E. FRONDOLIG, and C. L. FISCHER. *J. Ass. Advan. Med. Instrum.* In press.
4. DOLJANSKI, F., J. NAAMAN, and G. ZAJICEK. 1966. *Life Sci.* **5**:2095.
5. HARVEY, R. J. 1968. *Methods Cell Physiol.* **3**:1–23.
6. GUTMANN, J., G. HOFFMAN, and G. RUHENSTROTH-BAUER. 1966. *Bibl. Haematol.* **24**:42.
7. BREITMEYER, M. O., W. H. DENNIS, and G. PANTELEY. 1968. Evaluation of an On-Line System to Determine Volume Frequency Distributions of Biological Cells. 21st Annual Conference on Engineering in Medicine and Biology, Houston. 4.6.
8. HAPPEL, J., and H. BRENNER. 1965. Low Reynolds Number Hydrodynamics. Prentice-Hall, Inc., Englewood Cliffs, N. J. 512.
9. BURGERS, J. M. 1938. Second Amsterdam Report on Viscosity. North Holland Publishing Co., Amsterdam. 138.
10. JEFFERY, G. B. 1922. *Proc. Roy. Soc. London.* **A102**: 171.
11. CARSLAW, H. S., and J. C. JAEGER. 1959. Conduction of Heat in Solids. Clarendon Press, Oxford. 39.
12. GORIN, M., and S. VELICK. 1940. *J. Gen. Physiol.* **23**:753.